Lawrence Berkeley Laboratory
UNIVERSITY OF CALIFORNIA

Materials & Molecular Research Division

LBL--16296

DE84 002900

To be presented at the Brookhaven Conference, Advances in Soft X-Ray Science and Technology, Brookhaven National Laboratory, Upton, NY, October 17-20, 1983

GAS-PHASE PHOTOEMISSION WITH SOFT X-RAYS: CROSS SECTIONS AND ANGULAR DISTRIBUTIONS

D.A. Shirley, P.H. Kobrin, C.M. Truesdale, D.W. Lindle, T.A. Ferrett, P.A. Heimann, U. Becker, H.G. Kerkhoff, and S.H. Southworth

September 1983

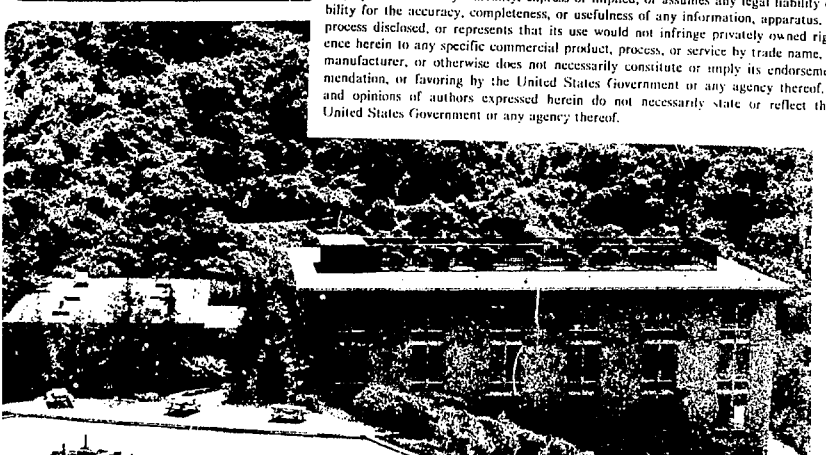

Prepared for the U.S. Department of Energy under Contract DE-AC03-76SF00098

Gas-phase photoemission with soft X-rays: Cross sections and angular distributions

D.A. Shirley, P.H. Kobrin,* C.M. Truesdale,** D.W. Lindle,
T.A. Ferrett, P.A. Heimann, U. Becker,† H.G. Kerkhoff,† and S.H. Southworth††

Materials and Molecular Research Division, Lawrence Berkeley Laboratory, and
Department of Chemistry, University of California, Berkeley, California 94720

Abstract

A summary is presented of typical gas-phase photoemission studies based on synchrotron radiation in the 50-5000 eV range, using beam lines at the Stanford Synchrotron Radiation Laboratory. Three topics are addressed: atomic inner-shell photoelectron cross sections and asymmetries, correlation peaks in rare gases, and core-level shape resonances in molecules. Photoelectron cross-section $\sigma(n\ell)$ and asymmetry-parameter $\beta(n\ell)$ studies in mercury vapor at photon energies up to 270 eV (up to 600 eV for β_{4f}) extend coverage of these parameters to $n\leq 5$ and $\ell\leq 3$. Comparison with Dirac-Slater and relativistic random-phase approximation calculations reveals systematic discrepancies. For example, distinct Cooper minima in $\sigma(n\ell)$ are observed but not predicted, while predicted $\beta(n\ell)$ values are typically too high. Correlation satellites have been studied for the K shells of helium ($h\nu$ = 68-90 eV), neon ($h\nu$ = 870-960 eV) and argon ($h\nu$ = 3200-3320 eV). In helium the n=2 satellite peak was shown to have mainly 2p character at threshold, and its asymmetry was measured through the autoionizing resonance region. Tentative evidence was obtained that the neon satellites are less intense near threshold than in the high-energy limit, and that their intensities stay constant or decrease with increasing energy near threshold. A new satellite was observed in argon at 24.6 eV which appears to increase in intensity with energy. Molecular core-level shape resonances were observed for the first time by photoemission, yielding $\sigma(h\nu)$ and $\beta(h\nu)$ for core levels from 180 eV binding energy (S 2p in SF_6 and OCS) through C 1s in CO, CO_2 and CF_4, N 1s in N_2 and NO, and O 1s in CO and CO_2 to 2490 eV (S 1s in SF_6). Several conclusions can be drawn about the photoelectron and Auger cross sections and asymmetry parameters.

Introduction

The field of gas-phase photoemission has expanded significantly with the use of high photon energies available with synchrotron radiation. Many interesting single-electron and multi-electron effects in atoms and molecules can be studied in this energy range. Centrifugal-barrier effects and Cooper minima in atoms and K-shell and L-shell shape resonances in small molecules are examples of one-electron effects that have been seen. Electron-correlation effects reveal themselves as correlation satellites in atomic inner-shell spectra, and energy-dependent measurements of their intensities yield valuable information about the dynamics of electron-electron interactions.

The experimental results presented here exhibit these effects as variations in the photoionization cross sections $\sigma(h\nu)$ and photoelectron angular-distribution asymmetry parameters $\beta(h\nu)$ of atomic and molecular subshells as a function of the photon energy $h\nu$. These two parameters are related by

$$\frac{d\sigma(h\nu)}{d\Omega} = \frac{\sigma(h\nu)}{4\pi}\left[1 + \beta(h\nu)P_2(\cos\theta)\right] , \qquad (1)$$

where $d\sigma(h\nu)/d\Omega$ is the differential cross section, θ is the angle between the photoelectron propagation direction and the polarization vector of the ionizing radiation, and $P_2(\cos\theta)$ is the second Legendre polynomial. Equation (1) is valid for linearly polarized radiation, a randomly oriented sample, and when electric-dipole transitions are dominant. Our measurements satisfy all of these requirements. Intensities of photoelectron peaks at $\theta = 54.7°$, where $P_2(\cos\theta)$ vanishes, suffice to determine relative partial cross sections. Simultaneous measurement at one additional angle (in this case 0°) determines the asymmetry parameters as well. The explicit dependence of the cross sections and asymmetry parameters on the photon energy is included in Eq. (1), but will be omitted throughout the remainder of this paper.

We will start with a discussion of photoionization in Hg to illustrate some single-electron effects in the 4f, 5d and 5p subshells. These results extend atomic measurements of cross sections and asymmetry parameters to subshells with $n\leq 5$ and $\ell\leq 3$. In the rare gases, He, Ne and Ar, we have studied K-shell satellite behavior as a function of photon energy to elucidate electron correlation. Finally, we present the first molecular K-shell shape-resonance effects measured for photoelectron asymmetry parameters.

Results and discussion

Mercury is the heaviest stable element with closed electronic subshells, and is of interest because both correlation and relativistic effects are important in Hg. The relative cross sections, subshell branching ratios, and angular-distribution asymmetry parameters were measured for the 4f, 5p, and 5d subshells from 50 to 270 eV photon energy (up to 600 eV for the 4f asymmetry parameter). Several theoretical studies have been performed on Hg. Among them are the Dirac-Slater (DS) calculation of Tambe and Manson[1] and the relativistic random-phase approximation (RRPA) calculation by Radojević and Johnson[2] which include predictions of each of the measured parameters for the three subshells.

Figure 1 shows the 5d cross-section data with earlier absorption measurements[3,4] and the DS[1] and RRPA[2,5] curves. Our data were scaled to the absorption results at 70 eV. Both the data and the calculated results show a 100-fold decrease from 50 eV to the Cooper minimum near 190 eV. Neither of the theoretical curves reproduce the minimum seen in the measured data. The 5d asymmetry parameter in Fig. 2 shows pronounced oscillations due to the shape resonance near threshold and the Cooper minimum.

The behavior of the 4f subshell is determined mainly by the "delayed onset" in the 4f → εg channel. Neither the RRPA nor the DS calculations agree well with our 4f cross-section results. The 4f asymmetry parameter is shown in Figure 3. While having the same general features, none of the theoretical curves quantitatively reproduce the data. Near 380 eV, β_{4f} shows a sudden increase that is probably caused by coupling with the 4d photoionization channels.

In the $5p_{3/2}$ and $5p_{1/2}$ subshells, Cooper minima were observed near 180 eV ($5p_{3/2}$) and 190 eV ($5p_{1/2}$). The branching ratio, $\sigma_{3/2}:\sigma_{1/2}$, showed a large deviation from the statistical value of 2 due to a kinetic-energy effect and the 18.5 eV spin-orbit splitting.

The experiments on Hg illustrate some interesting single-electron effects in atomic photoionization, but do not provide any insight into multi-electron processes that can occur via electron correlation. To learn more about multi-electron effects, we undertook a study of the photoionization of He because it provides the simplest example of electron correlation in atomic physics. Because correlation cannot occur in the hydrogen-like final state, theoretical studies of initial-state and continuum-state correlation effects are easier to interpret for the photoionization process.

We have studied the photoionization processes which leave the He^+ ion in the 1s, 2s or 2p final states. The 2s and 2p states are effectively degenerate in a photoemission experiment and thus are referred to under the encompassing term n=2. The n=2 states are produced entirely by electron correlation in the initial and continuum states (i.e they are correlation satellites of the 1s main line). Attempts to explain any results pertaining to the n=2 satellite must explicitly treat electron correlation in an accurate and consistent manner. For this reason, helium is an important system for testing theoretical approaches to the phenomenon of electron correlation.

Above 65.4 eV photon energy, photoelectrons corresponding to the n=2 final states are produced. By measuring the angular-distribution asymmetry parameter $\beta_{n=2}$ of these photoelectrons, we can estimate the relative probabilities of producing He^+ 2p and He^+ 2s as a function of energy because $\beta_{n=2}$ is a weighted average of β_{2p} and β_{2s}. Figure 4 shows the present results, several other measurements,[6-8] and two calculations for $\beta_{n=2}$.[6,9] Also shown is the β expected for He^+ 2p photoelectrons alone.[6,9] The asymmetry parameter for He^+ 2s is always two. The data indicate a predominance of the 2p final state near threshold that decreases with increasing energy. We also see that the two theoretical predictions differ significantly in the region near threshold. This discrepancy can be accounted for because the calculations treat electron correlation differently, and the threshold behavior of $\beta_{n=2}$ is sensitive to these differences.

In the energy region below the He^+ n=3 threshold, a series of Rydberg levels can be excited which autoionize to the 1s and n=2 final states. The autoionization phenomenon manifests itself as asymmetric profiles in the energy dependence of the partial cross sections and the asymmetry parameters. The effects on the n=2 states are shown in Figs. 5 and 6, where we see pronounced effects over the whole series of resonances. Results such as these provide further information on electron correlation, especially concerning how the satellite states interact with the resonance states. In favorable cases (He is one), individual dipole matrix elements can be derived from the data shown here and similar measurements for the He^+ 1s channel.

The other rare gases also are studied often to learn more about multi-electron (satellite) behavior. We report here the first photoelectron spectra taken near the 1s thresholds of Ne and Ar. New information was obtained about how satellites behave at low kinetic energies. Our results can be considered in terms of the relative energy parameter, ϵ/E_0, introduced by Wuilleumier and Krause,[10] where ϵ is the satellite photoelectron kinetic energy, and E_0 is the excitation energy, i.e. the binding energy separation of the satellite and the main line. The results of shake theory show that the satellite branching ratios to the main line should be constant at high values of ϵ/E_0. These experiments measured satellite branching ratios in the low and intermediate regions of ϵ/E_0 where shake theory does not apply.

Fig. 7 shows the branching ratios of the $3p_L$ and the unresolved $3p_U$ and $4p_L$ K-shell satellite states of Ne. In this measurement ϵ/E_0 varies from 0.1 to 1.4. For these small values of ϵ/E_0, the results tentatively suggest that the $3p_L$ relative intensity is decreasing as the energy increases, while the combined $3p_U$ and $4p_L$ relative intensity remains constant. Comparing these intensities near threshold to Gelius' measurement with Al K_α x-rays[11] implies that these satellite branching ratios increase in the intermediate region of ϵ/E_0. The relative intensity of the $3p_L$ satellite close to threshold is about 2.3(2)%, and falls 25% below the value at 1487 eV, whereas the sum of the $3p_U$ and $4p_L$ satellites is 3.2(2)% near threshold, 40% smaller than in Gelius' spectrum. Finally, though the many-body perturbation-theory calculation of Ishihara et al.[12] predicts the $2p \rightarrow 3s$ satellite to have a relative intensity of 5% near threshold, we did not observe it. At 25 eV kinetic energy, for example, we estimate that the $2p \rightarrow 3s$ intensity must be less than 0.7% of the main line.

The first photoelectron measurements in the region of the Ar 1s main line indicate the presence of a satellite at 24.6 eV excitation energy with a relative intensity of 6.0(5)%. Our measurement confirms the energy, 24.4 eV, and approximate intensity, 6.2%, predicted by Dyall[13] for the $[1s3p]4p(^1S)^2S_{1/2}$ state, where the brackets define the hole configuration. Dyall's calculation also suggests that there is a small contribution, 0.9% relative to the 1s main line, from other states which could not be resolved in our experiment. Fig. 8 displays the satellite relative intensity with ϵ/E_0 varying from 1.0 to 3.6. The relative intensity of the 4p satellite seems to increase with energy in this intermediate range of ϵ/E_0.

As well as the atomic studies discussed above, we have been studying molecular core-level shape-resonance effects. Shape resonances have been observed previously in photoabsorption and electron-impact measurements.[14-17] We report here the first observation of core-level shape resonances in photoemission, yielding partial cross sections and asymmetry parameters for Auger and photoelectrons from the C 1s, N 1s, O 1s, S 2p and S 1s subshells of several molecules.

The atomic-like C K-shell excitations in CO_2, CO, and CF_4 clearly demonstrate the effect of discrete transitions and shape resonances on the asymmetry parameters for C 1s photoelectrons and C(KVV) Auger electrons. Figure 9 shows σ and β for the C 1s photoelectrons in CO_2. The discrete transition at 290 eV is due to the C 1s $\rightarrow \pi^*$ resonance. The shape resonance is a 20 eV broad minimum in β and is located at 312 eV in the cross section. The effect has been attributed to the ℓ=2,3 channels in the C 1s $\rightarrow \sigma^*$ transition.[18]

For CO, similar effects are observed in the C 1s σ and β, though not as pronounced as in CO_2. Figure 10 shows the C(KVV) Auger cross section and asymmetry parameter for CO. A discrete π^* resonance appears below threshold as seen in the C(KVV) σ at 287.3 eV. The asymmetry parameter for an Auger transition can be described as

$$\beta_A(h\nu) = \beta_m(h\nu)A \qquad (2)$$

where $\beta_m(h\nu)$ is an orientation parameter and A is a constant factor dependent on the dynamics of the Auger-decay process. Dill et al.[19] have calculated $\beta_m(h\nu)$ using the multiple-scattering method (MSM) and find that $\beta_m(h\nu)$ for a $\sigma \rightarrow \pi^*$ transition should have a value of -1. We observe β near zero at 287.3 eV. One explanation for this behavior is that the A_j factors for the various Auger transitions of fractional strength f_j could have values that average $\beta_A(h\nu)$ to zero, according to

$$\beta_A(h\nu) = \beta_m(h\nu) \sum_j A_j f_j(h\nu) \qquad (-1/2 \leq A_j \leq 1) \qquad (3)$$

This near-zero cancellation of asymmetries at the discrete π^* resonance and the continuum σ^* resonance is difficult to accept. An alternate explanation is the "spectator" model, in which the excited electron retains the total orientation of the system in the π^* orbital, while the subsequent Auger decay shows only an isotropic distribution, as required by angular-momentum conservation. In general, the shape resonances have little or no effect in the continuum region on $\beta_A(h\nu)$ in all the molecules studied.

We have studied other shape resonances in a series of molecules and core-level subshells. Effects in the σ and β for CF_4 C(KVV) Auger and C 1s photoelectrons have been observed and are similar to those seen in CO and CO_2. The widths of the minimum in the C 1s β and the contrast ratio in the C 1s σ follow the ordering $CO<CF_4<CO_2$. The partial cross sections for the O(KVV) and the O 1s peaks of CO and CO_2 show the O 1s shape resonance. The N 1s subshell in N_2 and NO have been investigated for shape-resonance effects to extend these systematic studies to the N K-edge.

More recently we have undertaken a thorough investigation of the dramatic shape-resonance effects in SF_6. Our Auger and S 2p cross-section results confirm the presence of a discrete S 2p → $6a_{1g}$ transition at 171 eV and two continuum shape resonances (t_{2g}, e_g) at about 5 and 15 eV above threshold, respectively.[20] The S 2p β shows a strong minimum at the e_g shape resonance. In the S 1s subshell, the discrete S 1s → $6t_{1u}$ resonance was observed along with several very interesting smaller features in the S 1s continuum that also were seen in the photoabsorption spectrum.[21] Some of the continuum features are yet to be fully explained, although they may be associated with multiple excitations and shape-resonance effects.[20,22,23]

Acknowledgements

This work was supported by the Director, Office of Energy Research, Office of Basic Energy Sciences, Chemical Sciences Division of the U.S. Department of Energy under Contract No. DE-AC03-76SF00098. It was performed at the Stanford Synchrotron Radiation Laboratory, which is supported by the Department of Energy, Office of Basic Energy Sciences and the National Science Foundation, Division of Materials Research.

References

*Present address: Department of Chemistry, Pennsylvania State University, University Park, PA 16802.
**Present address: Research and Development Division, Corning Glass Works, Corning, NY 14831.
†Permanent address: Institute fur Strahlungs-und Kernphysik, Technische Universitat Berlin, W. Germany.
††Present address: National Bureau of Standards, Washington, DC 20234.

1. B.R. Tambe and S.T. Manson (private communication).
2. V. Radojević and W.R. Johnson, Phys. Lett. 92A, 75 (1982).
3. R.B. Cairns, H. Harrison, and R.I. Schoen, J. Chem. Phys. 53, 96 (1970).
4. J.L. Dehmer and J. Berkowitz, Phys. Rev. A 10, 484 (1974).
5. W.R. Johnson, V. Radojević, P. Deshmukh, and K.T. Cheng, Phys. Rev. A 25, 337 (1982).
6. J.M. Bizau, F. Wuilleumier, P. Dhez, D.L Ederer, T.N. Chang, S. Krummacher and V. Schmidt, Phys. Rev. Lett. 48, 588 (1982).
7. V. Schmidt, H. Derenbach and R. Malutzki, J. Phys. B 15, L523 (1982).
8. P. Morin, M.Y. Adam, I. Nenner, J. Delwiche, M.J. Hubin-Franskin and P. Lablanquie, Nucl. Instrum. Methods 208, 761 (1983).
9. V.L. Jacobs and P.G. Burke, J. Phys. B 5, L67 (1972).
10. F. Wuilleumier and M.O. Krause, Phys. Rev. A 10, 242 (1974).
11. U. Gelius, J. Electron Spectrosc. 5, 985 (1974).
12. T. Ishihara, J. Mizuno, and T. Watanabe, Phys. Rev. A 22, 1552 (1980).
13. K.G. Dyall (private communication).
14. R.B. Kay, Ph.E. Van der Leeuw, and M.J. Van der Wiel, J. Phys. B 10, 2513 (1973).
15. M. Tronc, G.C. King, R.C. Bradford, and F.H. Read, J. Phys. B 9, L555 (1976).
16. A. Hamnett, W. Stall, and C.E. Brion, J. Electron Spectrosc. 8, 367 (1976).
17. G.R. Wight, C.E. Brion, and M.J. Van der Wiel, J. Electron Spectrosc. 1, 457 (1973)
18. F.A. Grimm, Chem. Phys. 53, 71 (1980).
19. D. Dill, J.R. Swanson, S. Wallace, and J.L. Dehmer, Phys. Rev. Lett. 45, 1393 (1980).
20. J.L. Dehmer, J. Chem. Phys. 56, 4496 (1972).
21. R.E. LaVilla and R.D. Deslattes, J. Chem. Phys. 44, 4399 (1966).
22. F.A. Gianturco, C. Guidotti, and U. Lamanna, J. Chem. Phys. 57, 840 (1972).

23. J.L. Dehmer (private communication).
24. J.S. Shyu and S.T. Manson, Phys. Rev. A 11, 166 (1975).
25. F. Keller and F. Combet Farnoux, J. Phys. B 12, 2821 (1979).
26. G.R. Wight and C.E. Brion, J. Electron Spectrosc. 3, 191 (1974).
27. N. Padial, G. Csanak, B.V. McKoy, and P.W. Langhoff, Phys. Rev. A 23, 218 (1981).
28. R.R. Lucchese and B.V. McKoy, Phys. Rev. A 26, 1406 (1982).

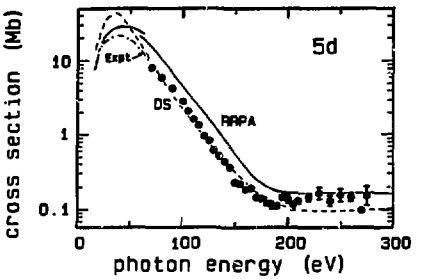

Fig. 1. Hg 5d cross section. Solid curves represent the RRPA calculations, Refs. 2 and 5. There is a discontinuity between the two calculations near 65 eV. Dashed curve represents the DS calculation, Ref. 1. Dashed-dotted curve is from absorption measurements, Refs. 3 and 4. Data were normalized to 8 Mb at 70 eV.

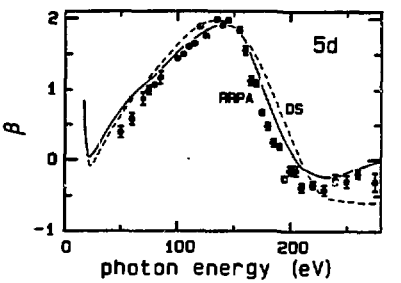

Fig. 2. Hg 5d angular-distribution asymmetry parameter. Solid curve is RRPA, Refs. 2 and 5; dashed curve, DS from Ref. 1.

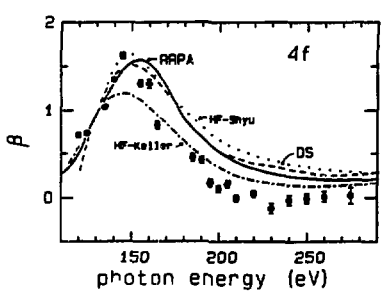

Fig. 3. Hg 4f asymmetry parameter. Theoretical curves; solid, RRPA, Ref. 2; dashed, DS theory, Ref. 1; dotted, HF, Ref. 24; dashed-dotted, HF, Ref. 25.

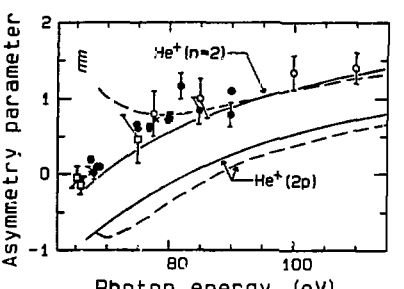

Fig. 4. Asymmetry parameter of the He^+ n=2 satellite as a function of photon energy. Experimental results; solid circles - present results; open circles - Ref. 6; X - Ref. 7; open squares - Ref. 8. Some error bars have been omitted for clarity. Theoretical curves; solid - Ref. 9; dashed - Ref. 6. Also shown are calculations of the asymmetry parameter for the 2p final state from Refs. 9 (solid) and 6 (dashed).

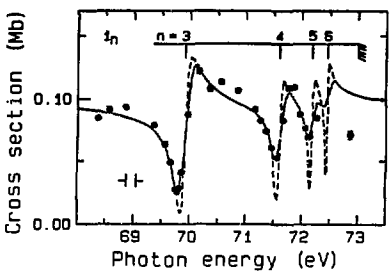

Fig. 5. Partial cross section of the He^+ n=2 satellite in the resonance region below the n=3 threshold. The solid curve is a fit to the data. The dashed curve is the same fit with the monochromator broadening removed.

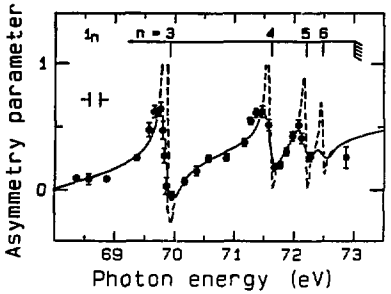

Fig. 6. Asymmetry parameter of the He^+ n=2 satellite in the resonance region below the n=3 threshold. Curves are as described in Fig. 5.

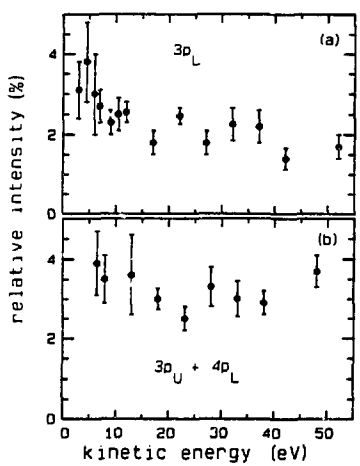

Fig. 7. The intensities of the $3p_L$ satellite (a), and the sum of the $3p_U$ and $4p_L$ satellites (b), relative to the intensity of the 1s main line (=100) of Ne, plotted versus satellite kinetic energy.

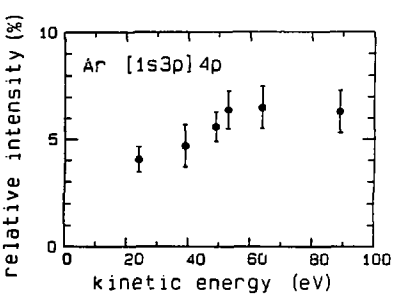

Fig. 8. Variation of the Ar 24.6 eV satellite intensity relative to the main line (=100) as a function of satellite kinetic energy.

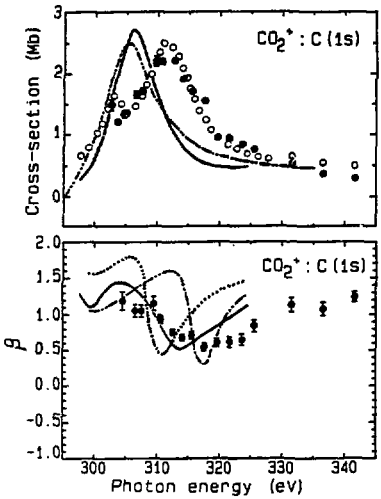

Fig. 9. C 1s results for CO_2. Filled circles - present results. Top panel: partial cross section. Open circles - electron-energy loss results, Ref. 26; dashed curve - STMT calculation, Ref. 27; solid curve - HF static-exchange calculation, Ref. 28. Bottom panel: asymmetry parameter. Solid curve - HF calculation, Ref. 28; dotted and dashed curves - localized- and unlocalized-hole MSMXα calculation, respectively, Ref. 18.

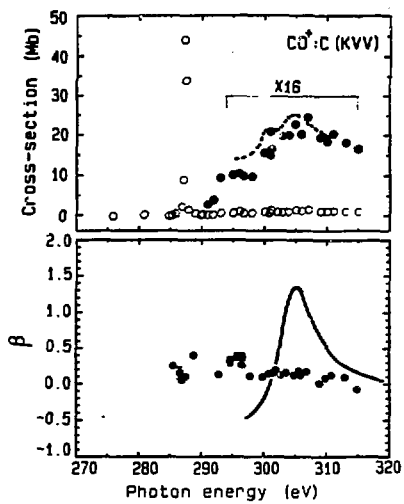

Fig. 10. C(KVV) Auger results for CO. Top panel: open circles - total Auger intensity scaled to results of Tronc et al., Ref. 15; filled circles - region above hν=290 eV, expanded 16 times; dashed curve - C 1s electron-ion coincidence measurements of Kay et al., Ref. 14. Bottom panel: filled circles - our asymmetry-parameter results; solid curve - orientation parameter $\beta_m(h\nu)$ calculated by Dill et al., Ref. 19.